

Intensity of Induced Earthquakes in Northeast British Columbia, Canada

Alireza Babaie Mahani^{1,2}, Stuart Venables³, Honn Kao⁴ , Ryan Visser⁴, Michelle Gaucher³, Ramin M. H. Dokht⁴, and Jeff Johnson³

Abstract

The damage potential of induced earthquakes associated with fluid injection is a major concern in hydrocarbon resource development. An important source of data for the assessment of damage is macroseismic intensity perceived by people and structures. In the Western Canada Sedimentary Basin (WCSB) where the occurrence of seismicity is mostly related to oil and gas activities, the collection of intensity data is incomplete. In this study, we present a comprehensive dataset gathered by the BC Oil and Gas Commission in the period 2016–2020. We assign intensities to individual felt reports according to the modified Mercalli intensity (MMI) scale and associate each MMI value to an earthquake. The isoseismal map of the largest earthquake in the Septimus region of northeast British Columbia is also provided using the compiled intensity dataset complemented with data from the U.S. Geological Survey and Natural Resources Canada “Did You Feel It?” systems along with the intensities converted from ground-motion amplitudes. We consider an approximate 10 km radius around the mainshock of 30 November 2018 earthquake with moment magnitude of 4.6 to be the meizoseismal area based on maximum intensities of 4–5. We also investigate the distance decay of intensity for shallow induced earthquakes in comparison with deeper natural events with the same magnitudes. Although intensities from shallow earthquakes (depth ≤ 5 km) can be higher than deep events (depth ≥ 10 km) at close distances (10–15 km), they tend to decrease abruptly at greater distances to become lower than deep events. The localization of large intensities from induced earthquakes within the meizoseismal area warrants special attention in future resource developments and call for systematic intensity data collection in the WCSB.

Cite this article as Babaie Mahani, A., S. Venables, H. Kao, R. Visser, M. Gaucher, R. M. H. Dokht, and J. Johnson (2021). Intensity of Induced Earthquakes in Northeast British Columbia, Canada, *Seismol. Res. Lett.* **XX**, 1–10, doi: [10.1785/SR202010037](https://doi.org/10.1785/SR202010037).

[Supplemental Material](#)

Introduction

Long before seismic sensors became available and deriving earthquake magnitude was possible, measuring the macroseismic intensity of shaking was the common practice after significant earthquakes. Although several intensity scales have been proposed in the last two centuries, the Rossi–Forel, Mercalli–Cancani–Sieberg (MCS), and the Medvedev–Sponheuer–Karnik were among the most referenced scales (Bath, 1973; Musson *et al.*, 2010). In 1931, Wood and Neumann modified the MCS scale and introduced the modified Mercalli intensity (MMI) scale. Further variations to the MMI scale were suggested by Stover and Coffman (1993) for the earthquakes occurred in the United States until 1989. The 1994 Northridge earthquake with moment magnitude (M_w) of 6.7 provided a wealth of intensity data for a relatively large earthquake. Dewey *et al.* (1995) used the criteria set by Wood and Neumann (1931) along with the amendments suggested by Stover and Coffman (1993) to draw isoseismal maps for the Northridge earthquake. Dengler and Dewey (1998) introduced

the concept of community decimal intensity (CDI) scale based on telephone-survey data by the Humboldt Earthquake Education Center and the U.S. Geological Survey (USGS) assigned MMI values following the Northridge earthquake. Furthermore, using a modified version of the CDI scale of Dengler and Dewey (1998), Wald *et al.* (1999) introduced the community internet intensity scale using responses obtained through internet. Community intensity is now reported routinely by the USGS after the occurrence of any felt earthquake with magnitude 1.9 or greater. USGS provides the community intensities for ZIP codes, cities, or geocoded boxes of 1 or 10 km sizes.

1. Mahan Geophysical Consulting Inc., Victoria, British Columbia, Canada; 2. Geoscience BC, Vancouver, British Columbia, Canada; 3. BC Oil and Gas Commission, Victoria, British Columbia, Canada; 4. Pacific Geoscience Center, Geological Survey of Canada, Sidney, British Columbia, Canada,  <https://orcid.org/0000-0001-9150-9416> (HK)

*Corresponding author: ali.mahani@mahangeo.com

© Seismological Society of America

With the exception of some relatively large earthquakes, intensity data for induced earthquakes within the Western Canada Sedimentary Basin (WCSB) have been limited compared with the wealth of data in the central and eastern United States (CEUS; e.g., [Hough, 2014](#); [Atkinson et al., 2018](#)). This is probably due to the low-population density and lack of systematic data collection in the WCSB. Nevertheless, due to the shallow depths of induced earthquakes and possible site effects, even small events in the magnitude range of 1–2 are reported by some residents who live close by. Near-field recordings of past induced earthquakes have shown relatively large peak ground accelerations in the order of $\sim 0.1g$ ($1g = 981 \text{ cm/s}^2$) at distances $< 5 \text{ km}$ from the epicenters of events with magnitudes as small as 3 ([Babaie Mahani and Kao, 2018](#)). These large ground accelerations, however, have short durations and are only localized at short distances from induced earthquakes. The occurrence of induced earthquakes has also been shown to alter the pre-existing hazard from natural tectonic earthquakes in areas with low-to-moderate background seismicity such as northeast British Columbia (NE BC) and western Alberta. Although induced seismicity can increase the hazard levels locally within a short-time period, it can have the effect of reducing the level of regional seismic hazard if the process of induced seismicity continues to occur over a long period of time and over a large area ([Atkinson, Ghofrani, and Assatourians, 2015](#); [Kao et al., 2018](#)). Shallow induced earthquakes with magnitudes > 5 have caused damage and casualties in other parts of the world such as Oklahoma, China, and South Korea ([Taylor et al., 2017](#); [Kang et al., 2019](#); [Liu and Zahradnik, 2020](#)). Because the largest induced earthquakes within the WCSB are approaching the M 5 range ([Atkinson, Assatourians, et al., 2015](#); [Eaton and Babaie Mahani, 2015](#); [Babaie Mahani et al., 2017, 2019](#); [Eaton et al., 2019](#); [Schultz et al., 2020](#)), understanding the level of intensities is an important task with regard to seismic risk assessment, especially at short distances from induced earthquakes.

In NE BC, a considerable number of the reports on felt seismicity come through the telephone and e-mail communications between local residents and the British Columbia Oil and Gas Commission (BCOGC). Although, at the time of writing this article, there is no standard questionnaire like the one used by the USGS or Natural Resources Canada (NRCAN), reports of felt seismicity can be useful in understanding the level and extent of shaking from induced earthquakes. This study would be the first to systematically and comprehensively review individual felt reports from all repository sources on induced seismicity in the WCSB. This document provides the analysis and overview of the intensities reported by the residents living in close proximity to oil and gas operations and earthquake epicenters, mostly within the Septimus region of NE BC. First, we explain our dataset and the process of assigning intensity levels to each felt report. We provide the intensity dataset in the supplemental material of this article for other researchers

working on the hazard and risk assessment of induced seismicity. We also provide the isoseismal map of the largest hydraulic-fracturing-induced event (M_w 4.6) that occurred within the Septimus region of NE BC on 30 November 2018. Distance decay of intensities from this event and other shallow induced earthquakes are investigated and compared with deeper natural earthquakes with similar magnitudes.

Intensity Dataset in NE BC

For the purpose of this study, we used the information from more than 400 reports of shaking intensity in the BCOGC dataset, gathered in the time period of 2016–2020. Most of the entries in this dataset include the occurrence of a felt event with no further information. However, especially for larger events, some description has been given such as hearing a bang, thud, or thump, the level of shaking (as weak or strong), duration (in seconds), shaking of the household items (pictures on the walls, dishes, furniture, and doors), and movement of some items such as chairs. For each felt entry, we assigned an intensity level based on the amount of detail that was given by people following the description of the MMI scale in [Dewey et al. \(1995\)](#). An MMI value of 2 was given for the reports that only mention the felt event without giving any description. The maximum MMI value was given as 5 for the reports that provide descriptions including moving chairs, crack in the wall, and objects falling.

After assigning an MMI value to each felt report, we searched to find the corresponding earthquake. For this purpose, we used four earthquake catalogs, including [Visser et al. \(2017\)](#) for period 2014–2016, [Visser et al. \(2020\)](#) for period 2017–2018, the 2019 catalog used by [Babaie Mahani \(2021\)](#), and the BC Seismic Research Consortium Seiscomp3 automatic solutions for 2020. For each felt entry with known location and timing (latitude and longitude of the resident and the reported date and time of the felt event), we calculated the time difference (in seconds) between that felt entry and all the events in the catalogs. In this step, we used various time difference thresholds (Δt) to look for events (0.5, 1, 2, 5, and 24 hr). We started by the shortest Δt (half an hour) and selected those events with time differences less than or equal to this threshold. We moved to a larger Δt if no event was found. After finding the events with a given Δt , if there was only one event, we then calculated the distance between this event and the felt location. If this distance was below a distance threshold (we chose a large distance threshold of 1000 km to include as many events as possible), we selected the event to be associated with the felt report. Otherwise, we moved to the next Δt . If there were more than one event according to a given Δt , we calculated the distances from all these events to the felt location and selected those below the distance threshold and, ultimately, chose the event with the maximum magnitude to be associated with the felt location. In case the felt location was known but the timing was vaguely specified (some of the felt incidents

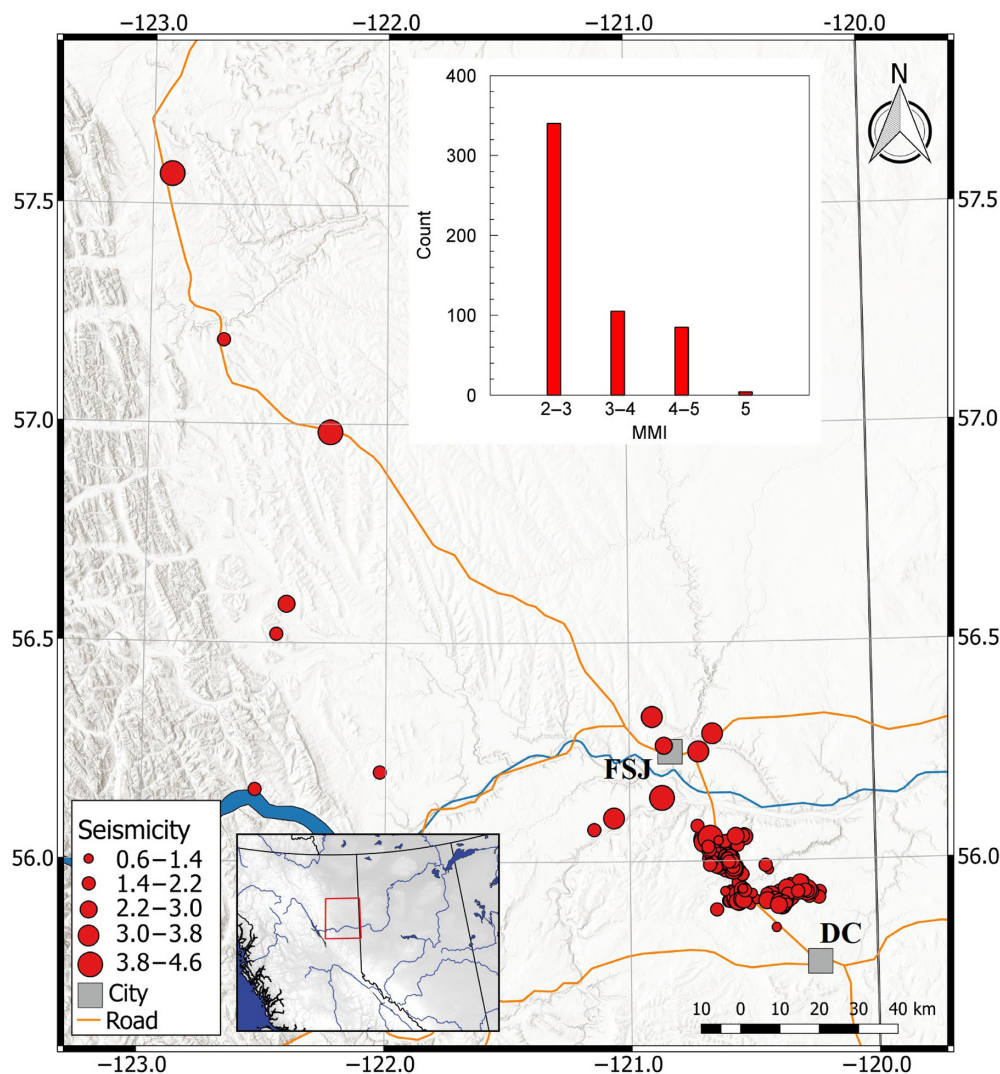


Figure 1. Map of northeast British Columbia and distribution of earthquakes for which intensities are available from the datasets of the BC Oil and Gas Commission, Natural Resources Canada, and U.S. Geological Survey (USGS). Histogram shows the number of felt reports for each intensity level. Inset shows the map of western Canada with the study area marked with a rectangle. DC, Dawson Creek; FSJ, Fort St. John; MMI, modified Mercalli intensity. The color version of this figure is available only in the electronic edition.

reported a general timing like “in the afternoon”), we searched for the events within one day of the felt report and applied the distance and magnitude criteria. For each felt entry, we also assigned a quality check (high or low) based on the Δt that was used to find the associated event. With the exception of seven entries for which the timings were vaguely specified and the associated events were searched within one day of the felt report, for all other entries, events were found within the shortest Δt (half an hour). Therefore, we assigned the low-quality check for those seven entries and the high-quality check for the rest of felt reports.

Besides the BCOGC felt dataset, we also used intensity data from two other sources. The first is the intensity dataset of

NRCan for several earthquakes in NE BC. The other dataset is the USGS community intensity data from the “Did You Feel It?” (DYFI) system for the M_w 4.6 earthquake on 30 November 2018 (Babaie Mahani *et al.*, 2019). Overall, the BCOGC dataset includes 339 individual felt entries associated with 222 earthquakes that occurred between 2016 and 2020 with magnitudes ranging from 0.6 to 4.6. The NRCan dataset includes 176 individual felt intensities for nine earthquakes between 2008 and 2018 with magnitudes ranging from 3.0 to 4.6. The USGS dataset includes intensities in different formats (versus distance or within geocoded boxes; see Data and Resources). Tables S1 and S2 in the supplemental material presents the intensity data from the BCOGC and NRCan datasets, respectively.

Figure 1 shows the distribution of earthquakes in NE BC for which intensities are available from the BCOGC, NRCan, and USGS datasets. Most of the events are concentrated in the southeast cluster in the Septimus region between Fort St. John (FSJ) and Dawson Creek (DC). Although events with magnitudes as low as 0.6 have been associated with some felt reports, most of the reports

are related to the M_w 4.6 earthquake on 30 November 2018. This event occurred in the Septimus region where hydraulic fracturing was in progress and was followed by two other earthquakes, less than an hour later, with M_w of 3.5 and 4.0 (Babaie Mahani *et al.*, 2019). Also shown in Figure 1 is the histogram of the number of felt reports for each MMI value. Most of the reports were assigned an MMI value between 2 and 3 with a few exceptions of MMI 5.

Isoseismal Map of the 30 November 2018 M_w 4.6 Earthquake

Figure 2 shows the intensity distribution for the M_w 4.6 earthquake on 30 November 2018, which is the largest event that has

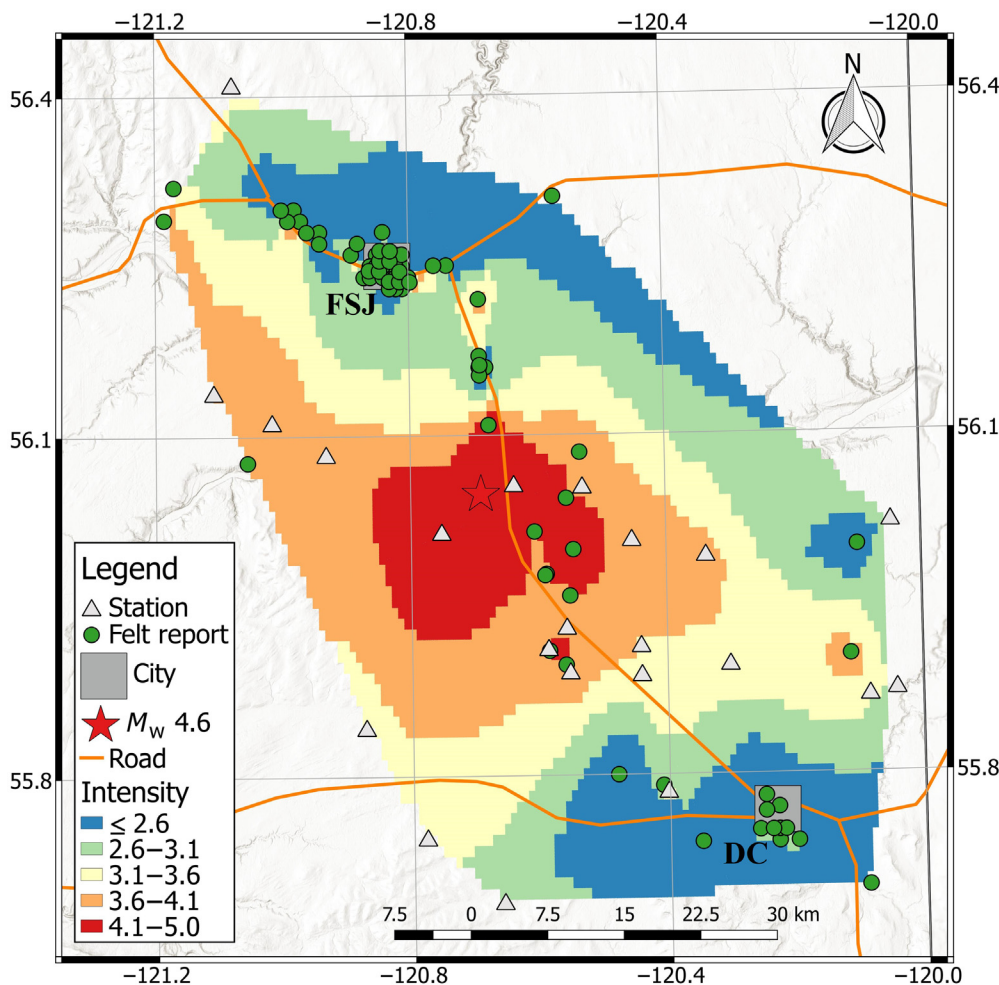


Figure 2. Isoseismal map showing intensity distribution for the induced earthquake on 30 November 2018 with moment magnitude (M_w) of 4.6 in the Septimus region of northeast British Columbia. DC, Dawson Creek; FSJ, Fort St. John. The color version of this figure is available only in the electronic edition.

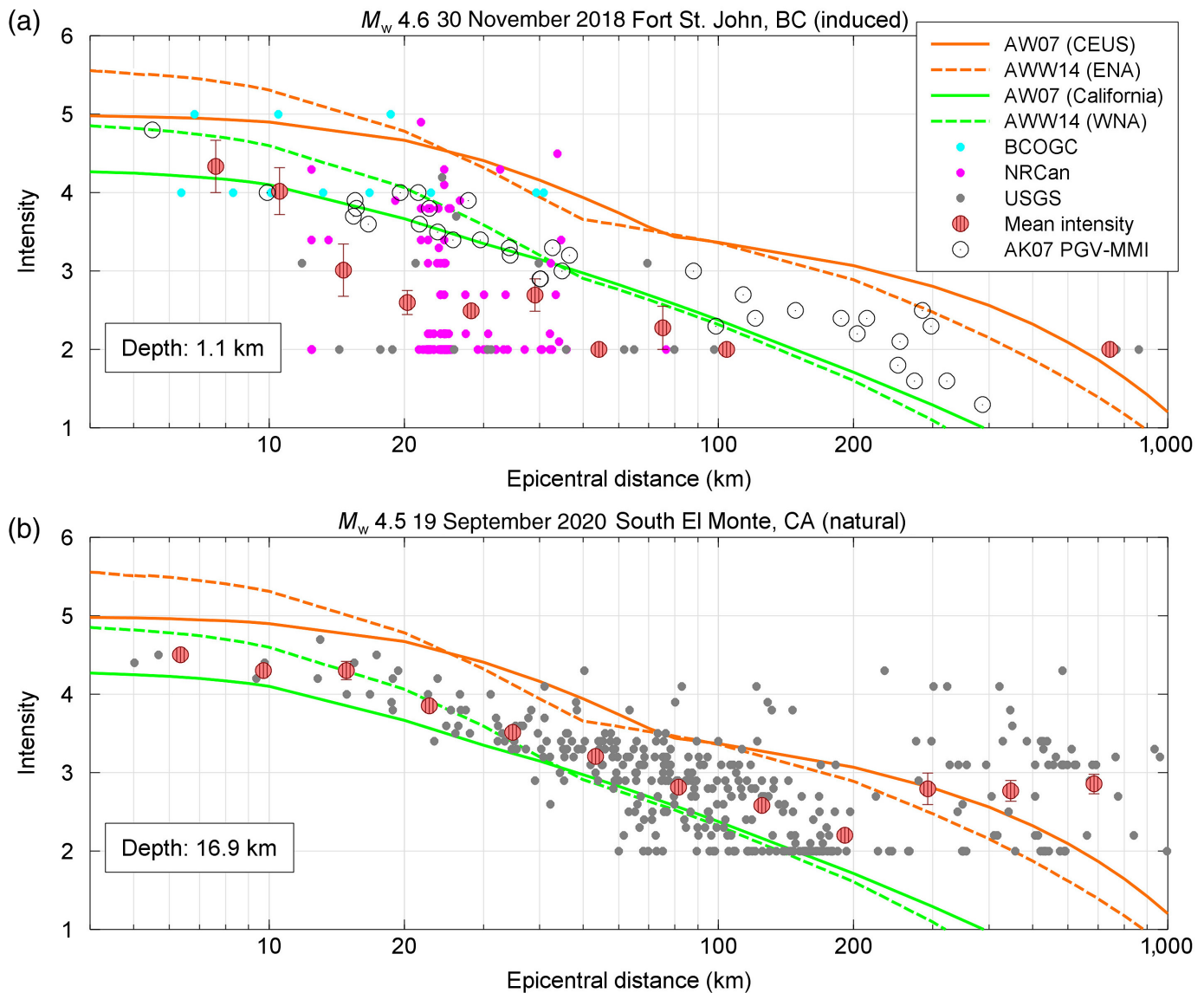
occurred in the Septimus region of NE BC during the instrumental period. We used intensity data from the BCOGC, NRCan, and USGS datasets (with community intensity ≥ 2 and with at least two observations in a 1 km geocoded box) to construct the isoseismal map shown in Figure 2. The M_w 4.6 earthquake was also recorded by many stations in the area that have been installed since 2013 for induced seismicity monitoring (along with the stations belonging to industry; Salas *et al.*, 2013; Salas and Walker, 2014; Babaie Mahani *et al.*, 2019). To add more data to our map, we also used the ground-motion intensity correlation equation (GMICE) proposed by Atkinson and Kaka (2007; hereafter, AK07) to convert the ground-motion amplitudes to the corresponding MMI values. Specifically, the geometric mean of the horizontal components of peak ground velocity (PGV) recorded at stations in the area and obtained by Babaie Mahani *et al.* (2019) was used in the calculation. The AK07 GMICE was developed based on MMI and

ground-motion pairs of earthquakes in California, central and northeastern United States, and southeastern Canada. To construct the isoseismal map, we used the natural neighbor interpolation technique in MATLAB (see Data and Resources) (function `griddata`). The maximum intensity values (4 and 5) shown in Figure 2 is similar to the values reported in other isoseismal maps produced for this earthquake for which limited intensity data were used (Babaie Mahani *et al.*, 2019; USGS; see Data and Resources). The addition of felt reports from the BCOGC, NRCan, and USGS datasets complemented with the wealth of intensity data converted from ground-motion amplitudes from public and research stations are clearly compatible with the epicenter of the M_w 4.6 earthquakes. Based on the area that experienced the intensities between 4 and 5, we consider an approximate 10 km radius around the mainshock to be the meizoseismal area of this earthquake. As will be explained in the next sections, higher intensities than natural earthquakes with similar

magnitudes are commonly observed in the meizoseismal area of induced earthquakes (within 10 km) due to their shallow depths, although intensities from induced events attenuate faster than those from natural earthquakes.

Intensity Decay of the 30 November 2018 M_w 4.6 Earthquake

Figure 3a shows the intensity versus epicentral distance for the M_w 4.6 earthquake. The observed intensities from the BCOGC, NRCan, and USGS datasets (solid small circles) are shown on this plot, along with their mean in distance bins (solid large circles). Overall, the intensities that were manually assigned to the BCOGC individual reports are higher than those from the USGS and NRCan in the distance range 10–40 km, which is consistent with the intensities obtained from field surveys in other areas (e.g., Hough, 2013; Frohlich *et al.*, 2014) compared with the community intensity measures reported by the USGS.



This is because the community intensities are average values of the intensities reported by the residents within a geographic area compared with the individual responses in the BCOGC dataset that can preferentially sample severe effects.

Despite the large scatter in the data, the average intensities are between 4 and 5 at close distances (<10 km) but decrease abruptly at larger distances. The observed cluster in the NRCan data can be partly due to the fact that the latitude and longitude of the locations were provided by only two decimal degrees (because of the privacy concerns), whereas coordinates provided by the BCOGC include up to six decimal degrees of precision. Also shown in Figure 3a are the predicted intensities for the corresponding magnitude using the Atkinson and Wald (2007; hereafter, AW07) intensity prediction equation (IPE) for the CEUS and California, and the updated IPE of Atkinson et al. (2014; hereafter, AWW14) for the eastern and western North America (ENA and WNA). Large open circles are the intensities converted from the recorded ground

Figure 3. (a) Intensity versus epicentral distance from the 30 November 2018 earthquake in the Septimus area of northeast British Columbia (south of Fort St. John, British Columbia, Fig. 1) with moment magnitude (M_w) of 4.6 and focal depth of 1.1 km. Small solid circles are the intensities from each dataset. Large solid circles are the mean intensity in distance bins with error bars showing the standard error. Lines are the predicted intensities from Atkinson and Wald (2007; referred as, AW07) and Atkinson et al. (2014; referred as, AWW14). AK07 is the intensity from peak ground velocity (PGV) using Atkinson and Kaka (2007) relationship. BCOGC, BC Oil and Gas Commission; CEUS, central and eastern United States; ENA, eastern North America; MMI, modified Mercalli intensity; NRCan, Natural Resources Canada; WNA, western North America. (b) Intensity versus epicentral distance from the 19 September 2020 M_w 4.5 South El Monte, California, earthquake with focal depth of 16.9 km. The color version of this figure is available only in the electronic edition.

motions of the M_w 4.6 earthquake using AK07 GMICE. The converted intensities match very well with the overall trend of the observed intensities, although they are consistently higher than the average intensities at distances above 10 km. One possible reason is the difference between intensity decay of induced and natural earthquakes, which is explained in the next section (the AK07 GMICE was developed using data from natural earthquakes). Moreover, the converted intensities from AK07 GMICE closely follow the AW07 and AWW14 prediction lines for California and WNA (also obtained using data from natural earthquakes) at distances below 100 km. At larger distances, the converted intensities lie above the prediction lines for California and WNA.

The intensities predicted by the CEUS and ENA IPEs are consistently larger than the observed and converted intensities and those predicted by the IPEs for California and WNA. Differences between the source characteristics of earthquakes (stress drop) and attenuation of seismic waves are the reasons for higher intensities in the eastern and northeast regions. Several studies have indicated higher stress drops and lower attenuation of high-frequency motions in the eastern and northeast regions compared with those in the west (including our study area; e.g., Atkinson and Wald, 2007; Babaie Mahani and Atkinson, 2012, 2013).

As can be seen from Figure 3a, data from the NRCAN and USGS only cover the distances above 10 km. At closer distances, the BCOGC dataset fills the data gap by providing valuable information regarding the level and extent of shaking, which is important for the purpose of seismic risk assessment of induced earthquakes that occur in proximity to residential buildings. Previous studies on intensity and damage potential of induced earthquakes in Oklahoma show that, within a distance of 10 km from epicenter, ground motions from events with M_w of ~ 4.5 exceed the damage threshold ($MMI = 6$) and some significant damage effects ($MMI = 7$) are also possible for events with $M_w > 4.8$ (Atkinson, 2020). It should be noted that the likelihood of the occurrence of earthquakes in the magnitude range of 4–5 is different between Oklahoma and NE BC. Although most moderate earthquakes in Oklahoma are caused by long-term disposal of wastewater, hydraulic fracturing has been the main cause of seismicity in NE BC. Compared to wastewater disposals, the affected area by hydraulic fracturing is limited to a few kilometers around the injection point. Proactive and reactive strategies have been undertaken by the operators and regulators in NE BC to prevent or reduce the effects of induced seismicity. These strategies include 5 km exclusion zones and real-time monitoring of operations to track the occurrence of seismicity and application of mitigation protocols (Atkinson, 2017).

Discussion

It is important to investigate the difference between observed intensities from shallow induced earthquakes and deeper

natural events. IPEs and conversion relationships (e.g., Atkinson and Kaka, 2007; Atkinson and Wald, 2007; Atkinson *et al.*, 2014) have been mostly based on data from natural events, and therefore their application can result in inaccurate estimation of intensities for induced earthquakes.

In Figure 3b, distance decay of intensity, taken from the USGS DYFI dataset, is shown for a natural earthquake in southern California (the 19 September 2020 M_w 4.5 South El Monte earthquake that occurred at a focal depth of 16.9 km). This moderate event generated more than 38,000 responses on the DYFI website with 391 geocoded community intensity values. Within the epicentral distance of 10 km, the average intensities (large solid circles) are compatible with the intensities caused by the M_w 4.6 induced earthquake in NE BC (Fig. 3a). At greater distances, average intensities from the California earthquake decay gently compared to the abrupt intensity reduction of the NE BC earthquake. This difference between intensities of natural and induced earthquakes has been systematically observed by other researchers using the wealth of intensity data for induced earthquakes in the CEUS, and it has been attributed to the difference in focal depth (Yenier and Atkinson, 2015; Atkinson *et al.*, 2018) and stress drop (Hough, 2014) as the controlling factors. Although Hough (2014) pointed out that at close distances intensities of shallow induced earthquakes are higher than deeper natural events, Atkinson *et al.* (2018) found that natural and induced earthquakes have similar average intensities within 10 km of the epicenter. Both Hough (2014) and Atkinson *et al.* (2018), however, found lower intensities for induced earthquakes at regional distances compared to natural tectonic events. Although Hough (2014) favored the interpretation that stress drop (which scales with the strength of high-frequency ground motion; Hanks and Johnston, 1992) is the controlling factor in the observed difference between intensities of natural and induced earthquakes, Atkinson *et al.* (2018) argued that focal depth is the controlling factor such that shallow events tend to have low-stress drop.

To test the generality of our observations depicted in Figure 3, we obtained more data from events with similar magnitudes and with sufficient number of intensities. Keeping the magnitude similar across these events, we can investigate the intensity decay between shallow and deep earthquakes. Our dataset includes nine shallow and six deep events with magnitudes in the range 4.5–4.7 (including those presented in Fig. 3). Here, we defined shallow and deep events as those with focal depth ≤ 5 km and ≥ 10 km, respectively. These events were chosen because each of them has at least 1000 intensity reports in the USGS DYFI dataset. Table 1 shows the parameters of the selected events. It is acknowledged that most of the shallow earthquakes are from Oklahoma and Kansas and therefore can be considered induced. For the purpose of this analysis, we did not subdivide the shallow earthquakes based on their cause. We note that to fully understand the controlling factors

TABLE 1

Parameters of the Earthquakes Used in This Study

Date (yyyy/mm/dd)	Time (UTC) (hh:mm:ss)	Latitude (°)	Longitude (°)	Depth (km)	Magnitude	Region
Shallow						
2010/04/06	04:12:21	32.59	-115.77	4.0	4.6	Mexico
2014/12/01	05:57:37	35.04	-111.73	5.0	4.7	Arizona
2015/07/27	18:12:15	35.99	-97.57	5.0	4.5	Oklahoma
2016/01/07	04:27:58	36.49	-98.73	4.1	4.7	Oklahoma
2018/04/09	10:22:20	36.22	-97.57	4.9	4.6	Oklahoma
2018/11/30	01:27:07	56.05	-120.69	1.1	4.6	British Columbia
2019/06/22	08:50:25	39.22	-99.43	3.0	4.6	Kansas
2020/01/19	19:08:42	38.02	-97.97	5.0	4.5	Kansas
2020/01/25	03:03:35	35.10	-116.99	3.1	4.6	California
Deep						
2013/03/11	16:56:06	33.50	-116.46	10.9	4.7	California
2018/03/23	03:09:39	40.43	-124.51	25.2	4.7	California
2019/07/12	09:51:38	47.87	-122.02	28.8	4.6	Washington
2020/03/18	19:12:24	40.75	-112.06	10.7	4.6	Utah
2020/05/10	22:07:40	33.02	-116.02	10.2	4.5	California
2020/09/19	06:38:47	34.04	-118.08	16.9	4.5	California

in observed intensities (focal depth and stress drop), one must normalize other variables beside magnitude (e.g., region: California vs. CEUS, cause: induced vs. natural).

We plotted the average intensity of the events presented in Table 1 as a function of epicentral distance in Figure 4. Intensity data from shallow events have larger event-to-event scattering, whereas data from deep events are tightly distributed. At close distances (<15 km), two of the shallow earthquakes show intensities >6 with three other events having intensities >5, compared to most intensities from deep events that show average intensities of <5. To see the difference between intensities of shallow and deep earthquakes across the entire distance range, we computed intensity decay through fitting a simple line to the data at different cutoff distances. We regressed the data against the equation:

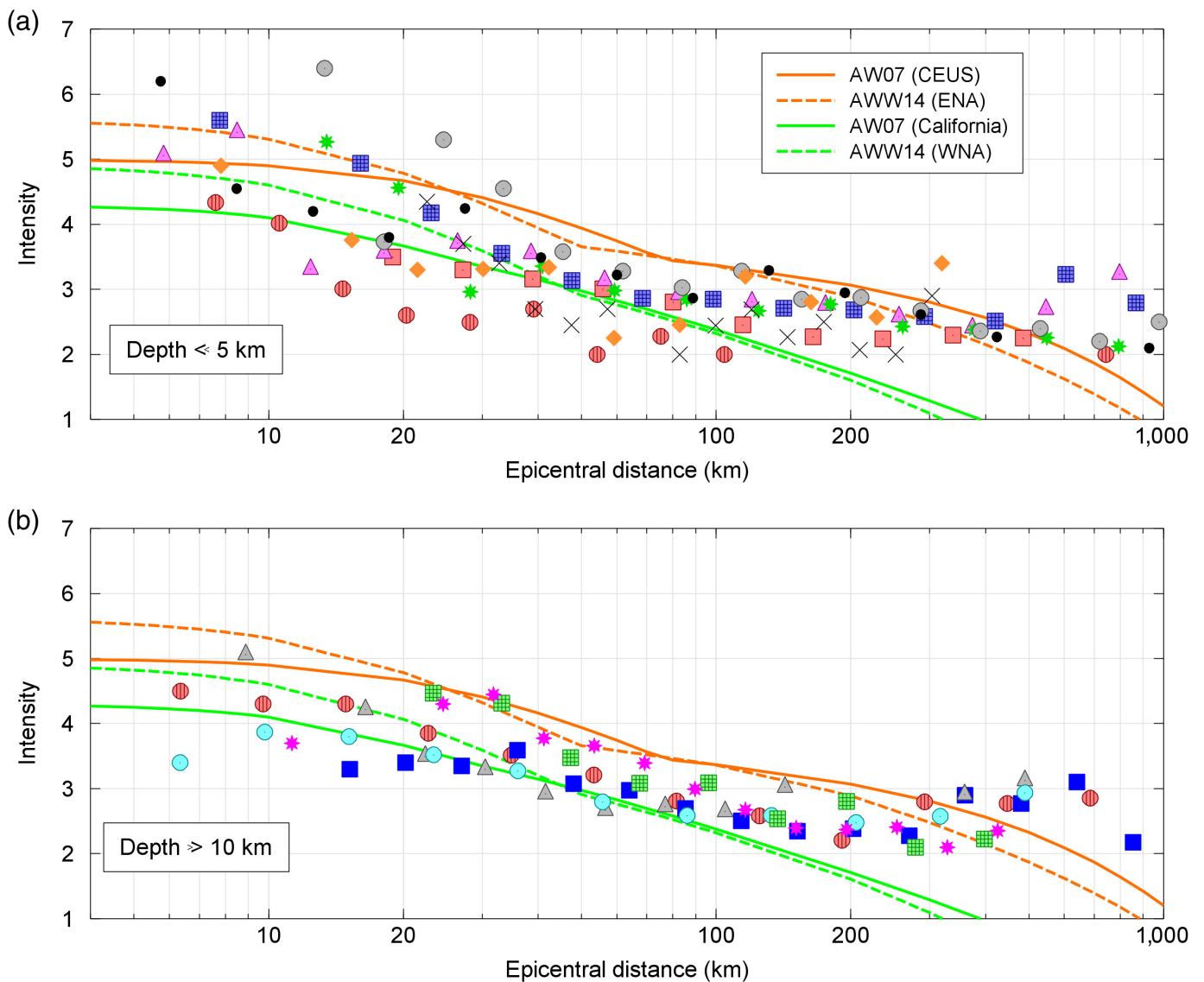
$$I = c + eD, \quad (1)$$

in which I and D are intensity and epicentral distance, respectively, and c and e are the parameters to be determined by the least-squares regression. Figure 5 shows the slope (e) of equation (1) versus the cutoff distance. To ensure reliable results for each earthquake, we obtained the slope if there were at least five observations below each cutoff distance. From Figure 5 it is clear that the average slope for shallow earthquakes varies

significantly, from -0.4 at the distance of 10 km to ~ -0.1 at the distance of 20 km. The slope becomes stable beyond 20 km. On the other hand, the slope for deep earthquakes does not vary much below the distance of 40 km with an average value close to the zero line. For the cutoff distances of 40 km and greater, both the shallow and deep events show similar decay in intensities with distance. Results shown in Figures 4 and 5 emphasize this notion that although ground-motion amplitudes from shallow induced earthquakes can be higher than the damage threshold (MMI 5 and 6) at close distances compared to deep natural events with similar magnitudes, they tend to decrease abruptly at larger distances and become lower than deep natural events. Localization of the higher damage potential of induced earthquakes than natural events at close distances is an important takeaway message from this study that should not be overlooked in hydrocarbon resource development.

Conclusions

In this study, we provided a comprehensive dataset of macroseismic intensity distribution from induced earthquakes that occurred in NE BC between 2016 and 2020. For each felt report gathered by the BC Oil and Gas Commission, we assigned an intensity value according to the MMI scale based on descriptions given in the report. Overall, our dataset includes 339 MMI values



associated with earthquakes in the magnitude range of 0.6–4.6, complemented with intensity reports from the USGS and NRCan DYFI datasets. Using the compiled datasets, we constructed the isoseismal map of the largest hydraulic-fracturing-induced earthquake in the WCSB that occurred on 30 November 2018 with a moment magnitude (M_w) of 4.6. The approximate extent of the maximum intensities (4–5) has a radius of 10 km. Quantitative analysis of the distance decay of intensity from events with M_w between 4.5 and 4.7 shows that, at close distances (10–15 km), shallow (depth ≤ 5 km) events generate higher intensities than deep (depth ≥ 10 km) earthquakes. At greater distances, however, intensities from shallow earthquakes drop significantly and become lower than deep events. Observation of high intensities above the damage threshold in the meizoseismal area of shallow induced earthquakes is an important factor that should not be overlooked in future hydrocarbon resource developments. Comprehensive analysis of background seismicity (e.g., maximum event magnitude, ground-motion amplitudes, and duration), effect of site

Figure 4. Average intensity of (a) shallow (depth ≤ 5 km) and (b) deep (≥ 10 km) earthquakes versus distance (Table 1). AW07 and AWW14 are the intensity prediction equations of Atkinson and Wald (2007) and Atkinson et al., 2014, respectively. CEUS, central and eastern United States; ENA, eastern North America; WNA: western North America. The color version of this figure is available only in the electronic edition.

condition, population density, and infrastructure in the area should be performed prior to the start of injections.

Data and Resources

Data for the 30 November 2018 earthquake in northeast British Columbia (NE BC) can be obtained from <https://earthquake.usgs.gov/earthquakes/eventpage/us1000hy6d/executive>. The Matlab is available at www.mathworks.com/products/matlab. All websites were last accessed in April 2021. The supplemental material of this article includes intensity data from the British Columbia Oil and Gas Commission (BCOGC) and Natural Resources Canada (NRCan) datasets.

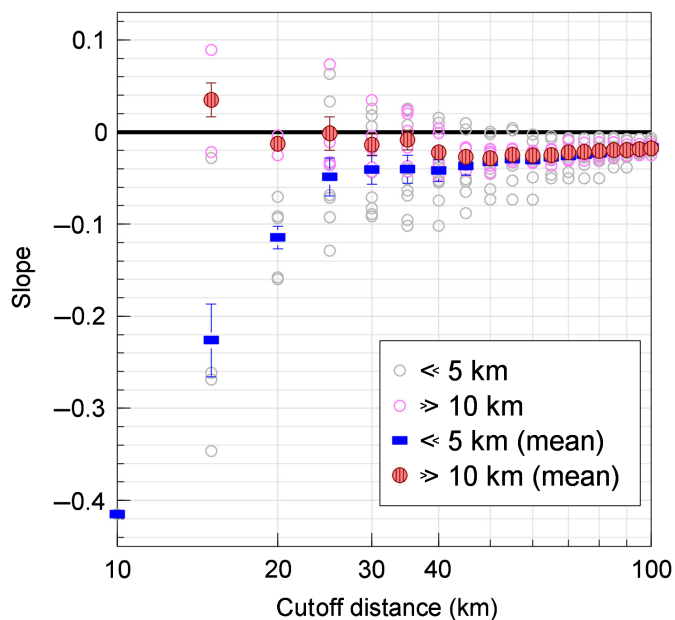


Figure 5. Slope (equation 1) of intensity decay versus cutoff distance for shallow (depth ≤ 5 km) and deep (depth ≥ 10 km) earthquakes (Table 1). Open circles are the individual data for each earthquake whereas solid symbols are the mean of slope from all the earthquakes. Error bars are the standard error of the mean. The color version of this figure is available only in the electronic edition.

Declaration of Competing Interests

The study presented in this article is a collaboration among private and public sectors involved in research and monitoring of induced seismicity in British Columbia. Funding for this study was provided by several agencies. The BC Oil and Gas Commission, as the provincial regulatory agency of oil and gas activities, provided in-kind support. Additional funding from Geoscience BC (public nonprofit organization) was also provided via the BC Seismic Research Consortium, which is supported by the Canadian Association of Petroleum Producers (oil and gas companies), and the BC Oil and Gas Research and Innovation Society. The induced seismicity research team at the Geological Survey of Canada, which is the federal authority for earthquake monitoring in Canada, provided funding for the enhancement of the seismic network. The corresponding author is represented by Mahan Geophysical Consulting Inc., which is a private consulting firm involved, as consultant, in the Geoscience BC Induced Seismicity Monitoring Project in British Columbia.

Acknowledgments

The authors would like to thank the SRL Editor-in-Chief, Allison Bent, and two reviewers, Susan Hough, and Bruce Worden, for their constructive comments on this work. This work was partially supported by Geoscience BC, BC Oil and Gas Research and Innovation Society, the Canadian Association of Petroleum

Producers, the Natural Sciences and Engineering Research Council of Canada, and the Environmental Geoscience Program of Natural Resources Canada (NRCan).

References

- Atkinson, G., K. Assatourians, B. Cheadle, and W. Greig (2015). Ground motions from three recent earthquakes in western Alberta and northeastern British Columbia and their implications for induced-seismicity hazard in eastern regions, *Seismol. Res. Lett.* **86**, 1022–1031.
- Atkinson, G. M. (2017). Strategies to prevent damage to critical infrastructure due to induced seismicity, *Facets* **2**, 374–394.
- Atkinson, G. M. (2020). The intensity of ground motions from induced earthquakes with implications for damage potential, *Bull. Seismol. Soc. Am.* **110**, 2366–2379.
- Atkinson, G. M., and S. I. Kaka (2007). Relationships between felt intensity and instrumental ground motion in the central United States and California, *Bull. Seismol. Soc. Am.* **97**, 497–510.
- Atkinson, G. M., and D. J. Wald (2007). “Did you feel it?” intensity data: A surprisingly good measure of earthquake ground motion, *Seismol. Res. Lett.* **78**, 362–368.
- Atkinson, G. M., H. Ghofrani, and K. Assatourians (2015). Impact of induced seismicity on the evaluation of seismic hazard: Some preliminary considerations, *Seismol. Res. Lett.* **86**, 1009–1021.
- Atkinson, G. M., D. Wald, C. B. Worden, and V. Quitoriano (2018). The intensity signature of induced seismicity, *Bull. Seismol. Soc. Am.* **108**, 1080–1086.
- Atkinson, G. M., C. B. Worden, and D. J. Wald (2014). Intensity prediction equations for North America, *Bull. Seismol. Soc. Am.* **104**, 3084–3093.
- Babaie Mahani, A. (2021). Seismic b-value within the Montney Play of Northeast British Columbia, Canada, *Can. J. Earth Sci.*, doi: [10.1139/cjes-2020-0157](https://doi.org/10.1139/cjes-2020-0157).
- Babaie Mahani, A., and G. M. Atkinson (2012). Evaluation of functional forms for the attenuation of small-to-moderate-earthquake response spectral amplitudes in North America, *Bull. Seismol. Soc. Am.* **102**, 2714–2726.
- Babaie Mahani, A., and G. M. Atkinson (2013). Regional differences in ground-motion amplitudes of small-to-moderate earthquakes across North America, *Bull. Seismol. Soc. Am.* **103**, 2604–2620.
- Babaie Mahani, A., and H. Kao (2018). Ground motion from M 1.5 to 3.8 induced earthquakes at hypocentral distance < 45 km in the Montney play of northeast British Columbia, Canada, *Seismol. Res. Lett.* **89**, 22–34.
- Babaie Mahani, A., H. Kao, G. M. Atkinson, K. Assatourians, K. Addo, and Y. Liu (2019). Ground motion characteristics of the 30 November 2018 injection-induced earthquake sequence in Northeast British Columbia, Canada, *Seismol. Res. Lett.* **90**, 1457–1467, doi: [10.1785/0220190040](https://doi.org/10.1785/0220190040).
- Babaie Mahani, A., R. Schultz, H. Kao, D. Walker, J. Johnson, and C. Salas (2017). Fluid injection and seismic activity in the Northern Montney Play, British Columbia, Canada, with special reference to the 17 August 2015 Mw 4.6 Induced Earthquake, *Bull. Seismol. Soc. Am.* **107**, 542–552, doi: [10.1785/0120160175](https://doi.org/10.1785/0120160175).
- Bath, M. (1973). *Introduction to Seismology*, John Wiley & Sons, New York, New York, 395 pp.

- Dengler, L. A., and J. W. Dewey (1998). An intensity survey of households affected by the Northridge, California, earthquake of 17 January 1994, *Bull. Seismol. Soc. Am.* **88**, 441–462.
- Dewey, J. W., B. G. Reagor, L. Dengler, and K. Moley (1995). Intensity distribution and isoseismal maps for the Northridge, California, earthquake of January 17, 1994, *U.S. Geol. Surv. Open-File Rept.* 95-92, 37 pp.
- Eaton, D. W., and A. Babaie Mahani (2015). Focal mechanisms of some inferred induced earthquakes in Alberta, Canada, *Seismol. Res. Lett.* **86**, 1078–1085.
- Eaton, D. W., A. Babaie Mahani, R. Salvage, H. Kao, and M. van der Baan (2019). A tale of three earthquakes: New insights into fault activation in light of recent occurrences in western Canada, *New Directions in Geosciences for Unconventional Resources*, 15–17 October 2019, Banff, Canada.
- Frohlich, C., W. Ellsworth, W. A. Brown, M. Brunt, J. Luetgert, T. MacDonald, and S. Walter (2014). The 17 May 2012 M 4.8 earthquake near Timpson, east Texas: An event possibly triggered by fluid injection, *J. Geophys. Res.* **119**, 581–593.
- Hanks, T. C., and A. C. Johnston (1992). Common features of the excitation and propagation of strong ground motion for North American earthquakes, *Bull. Seismol. Soc. Am.* **82**, 1–23.
- Hough, S. E. (2013). Spatial variability of “Did You Feel It?” intensity data: Insights into sampling biases in historical earthquake intensity distributions, *Bull. Seismol. Soc. Am.* **103**, 2767–2781.
- Hough, S. E. (2014). Shaking from injection-induced earthquakes in the central and eastern United States, *Bull. Seismol. Soc. Am.* **104**, 2619–2626.
- Kang, S., B. Kim, S. Bae, H. Lee, and M. Kim (2019). Earthquake-induced ground deformations in the low-seismicity region: A case of the 2017 M5.4 Pohang, South Korea, earthquake, *Earthq. Spectra* **35**, 1235–1260.
- Kao, H., R. D. Hyndman, Y. Jiang, R. Visser, B. Smith, A. Babaie Mahani, L. J. Leonard, H. Ghofrani, and J. He (2018). Induced seismicity in western Canada linked to tectonic strain rate: Implications for regional seismic hazard, *Geophys. Res. Lett.* **45**, 11,104–11,115.
- Liu, J., and J. Zahradnik (2020). The 2019 Mw 5.7 Changning earthquake, Sichuan Basin, China—A shallow doublet with different faulting styles, *Geophys. Res. Lett.* **47**, e2019GL085408, doi: [10.1029/2019GL085408](https://doi.org/10.1029/2019GL085408).
- Musson, R. M. W., G. Grünthal, and M. Stucchi (2010). The comparison of macroseismic intensity scales, *J. Seismol.* **14**, 413–428.
- Salas, C. J., and D. Walker (2014). Update on regional seismograph network in Northeastern British Columbia (NTS 094C, G, I, O, P), *Geoscience BC Summary of Activities 2013*, *Geoscience BC, Rept.* 2014-1, 123–126.
- Salas, C. J., D. Walker, and H. Kao (2013). Creating a regional seismograph network in Northeast British Columbia to study the effect of induced seismicity from unconventional gas completions (NTS 094C, G, I, O, P), *Geoscience BC Summary of Activities 2012*, *Geoscience BC, Rept.* 2013-1, 131–134.
- Schultz, R., R. J. Skoumal, M. R. Brudzinski, D. Eaton, B. Baptie, and W. Ellsworth (2020). Hydraulic fracturing-induced seismicity, *Rev. Geophys.* **58**, e2019RG000695, doi: [10.1029/2019RG000695](https://doi.org/10.1029/2019RG000695).
- Stover, C. W., and J. L. Coffman (1993). *Seismicity of the United States, 1568-1989 (revised)*, United States Government Printing Office, Washington, D.C., 424 pp.
- Taylor, J., M. Celebi, A. Greer, E. Jampole, A. Masroor, S. Melton, D. Norton, N. Paul, E. Wilson, and Y. Xiao (2017). M5.0 Cushing, Oklahoma, USA Earthquake on November 7, 2016, *EERI Earthquake Reconnaissance Team Rept.*, 25 pp., available at http://learningfromearthquakes.org/2016-09-03-oklahoma/images/2016_09_03_oklahoma/pdfs/Oklahoma-EERI-Recon-Report-2017-02-15-Finalized.pdf (last accessed April 2021).
- Visser, R., H. Kao, B. Smith, C. Goerzen, B. Kontou, R. M. H. Dokht, J. Hutchinson, F. Tan, and A. Babaie Mahani (2020). A comprehensive earthquake catalogue for the Fort St. John-Dawson Creek Region, British Columbia, 2017-2018, *Geol. Surv. Can. Open-File Rept.* 8718, 28 pp., doi: [10.4095/326015](https://doi.org/10.4095/326015) (open access).
- Visser, R., B. Smith, H. Kao, A. Babaie Mahani, J. Hutchinson, and J. McKay (2017). A comprehensive earthquake catalogue for Northeastern British Columbia and Western Alberta, 2014–2016, *Geol. Surv. Can. Open-File Rept.* 8335, 28 pp., doi: [10.4095/306292](https://doi.org/10.4095/306292) (open access).
- Wald, D. J., V. Quitoriano, L. A. Dengler, and J. W. Dewey (1999). Utilization of the internet for rapid community intensity maps, *Seismol. Res. Lett.* **70**, 680–697.
- Wood, H. O., and F. Neumann (1931). Modified Mercalli intensity scale of 1931, *Bull. Seismol. Soc. Am.* **21**, 277–283.
- Yenier, E., and G. M. Atkinson (2015). Regionally adjustable generic ground-motion prediction equation based on equivalent point-source simulations: Application to central and eastern North America, *Bull. Seismol. Soc. Am.* **105**, 1989–2009.

Manuscript received 2 February 2021

Published online 19 May 2021